ELSEVIER

Surface Science 440 (1999) 151–162

surface science

www.elsevier.nl/locate/susc

Site selective probe of the desorption of CO from Pd(111) by sum frequency generation and Fourier transform IR: a comparison of thermal and laser desorption

Serge Carrez [a], Bogdan Dragnea [a], Wan Quan Zheng [b], Henri Dubost [a], Bernard Bourguignon [a,*]

[a] *Laboratoire de Photophysique Moléculaire du CNRS, Bâtiment 210 Université de Paris-Sud, 91405 Orsay Cedex, France*
[b] *Laboratoire pour l'Utilisation du Rayonnement Electromagnétique (LURE), Bâtiment 209 Université de Paris-Sud, 91405 Orsay Cedex, France*

Received 23 April 1999; accepted for publication 19 June 1999

Abstract

The laser induced desorption of CO from Pd(111) at 308 nm and 532 nm is compared to the thermal desorption by recording FTIR and SFG spectra of the CO molecules remaining on the surface. There is no photodesorption from a fully ordered CO layer. However, when the CO layer is adsorbed below 270 K, extra sites (assigned to antiphase domain boundaries) appear in addition to the normal sites (assigned to domains), and the photodesorption occurs selectively from the extra sites. The relative stability of the various sites is similar under heating and under laser exposure, but the numerical calculation of laser heating and of the corresponding thermal desorption shows that laser heating cannot account for the observed photodesorption.

Keywords: Carbon monoxide; Chemisorption; IR absorption spectroscopy; Low index single crystal surfaces; Palladium; Solid gas interface; Sum frequency generation; Surface defects

1. Introduction

In recent years, it was shown that the energy of laser excited electrons at a solid surface can be channelled into the motion of adsorbates and induce surface modifications like photodesorption, photodissociation, and reactions among coadsorbates. The emphasis was on demonstrating experimentally that these effects are non-thermal [1]. This has been done in many cases by measuring the distribution of the translational, vibrational and rotational energies of the desorbed molecules using the very sensitive technique of resonantly enhanced multiphoton ionisation (REMPI). Although REMPI is the most sensitive probe of photodesorption and provides direct information on the desorption dynamics through the measurement of the energy released in the translational and internal degrees of freedom of the desorbed molecules, measuring vibrational spectra of the adsorbate is useful to provide complementary information on photodesorption, because it shows without ambiguity which of the adsorption sites are sensitive to photoexcitation. Site selective effects, if present, may have practical applications, like the preparation of a surface where only certain

* Corresponding author. Fax: +33-1-60-19-25-93.
E-mail address: bernard.bourguignon@ppm.u-psud.fr (B. Bourguignon)

0039-6028/99/$ – see front matter
PII: S0039-6028(99)00781-5

sites would be occupied by adsorbates. They may also provide indications about the topology of the potential energy surfaces (PES). This is important because experimental information on ground and excited states PES is very poor. This is because photoelectrons in a solid lose their initial energy at a very short time scale ($\sim$1 fs) due to electron–electron collisions, before desorption may occur. Thus, desorption is induced by electrons having a wide dispersion of energy.

A site selective method was employed in a few cases to probe the laser action. For CO on Pt(100), a laser was used to produce strong heating (870 K), and this resulted in the interconversion of a fraction of the linearly bonded CO to bridge sites, as observed by Fourier transform infrared (FTIR) spectroscopy [2]. On Pt(111), the non-thermal desorption of CO and CO^+ is observed to be site selective [3]. NO is selectively photodesorbed from the on-top sites on Ag(111), Cu(111) [4], and Pt(111) [5–7], while it is photodissociated on the bridge sites of Pt(111) [8]. On the Si(111) 7×7 surface, preferential photodesorption of Si adatoms and chlorinated adatoms occurs upon irradiation at 248 nm and 193 nm, respectively [9,10], and 355 and 266 nm [7], as shown by STM. A few cases were reported where non-thermal site effects were inferred using indirect methods. For example, in the case of O_2 on Pd(111), interconversion between sites, and site-dependent desorption cross-sections, were deduced from temperature programmed desorption (TPD) of the undesorbed molecules [11].

CO on Pd(111) may adsorb on a variety of adsorption sites, depending on the surface coverage. The saturation coverage itself depends on the surface temperature because the adsorption energy decreases with coverage, as a result of the repulsive CO–CO interactions [12]. The order of stability of the adsorption sites for an isolated CO molecule on Pd(111) is three-fold hollow > bridge > linear. Thus, three-fold hollow sites are preferred at low coverage [$\leq$0.33 monolayer (ML), where 1 ML = 1.53×10^{15} cm^{-2}, the density of Pd atoms on the (111) surface]. Between 0.33 and 0.50 ML, CO molecules occupy bridge sites. Between 0.5 and 0.6 ML, CO remains in bridge sites but with a compressed structure that involves large unit cells

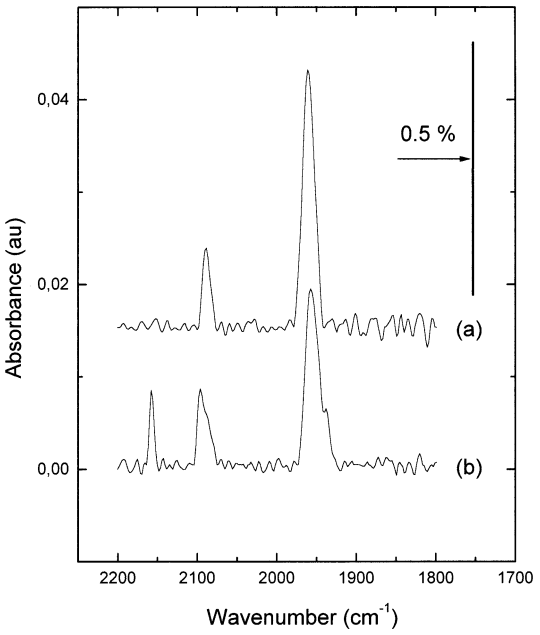

Fig. 1. FTIR spectra of CO on Pd(111) when (a) the CO layer is fully ordered, and when (b) the CO layer is adsorbed below $\sim$270 K. The conditions of adsorption are (a) annealing to 330 K and cooling to 170 K under a CO pressure of 10^{-7} mbar, (b) unannealed surface obtained by direct adsorption at 170 K at a CO pressure of 10^{-7} mbar. Both spectra are recorded under 10^{-7} mbar. Note the reduction in peak of the bridge sites at $\sim$1950 cm^{-1}, and the broadening in peak of the linear sites at 2083–2093 cm^{-1}, in (b) with respect to (a).

with an increased density at the cell boundaries [13]. Between 0.60 and 0.66 ML, a combination of linear and bridge sites is observed. Above 0.66 ML, the structure consists of three-fold hollow and linear sites. The 'ultimate' saturation coverage (in the absence of gas phase CO) of 0.75 ML is obtained at $\sim$100 K [12]. The adsorption energy decreases with coverage from 1.5 to 0.26 eV [12,14].

In our experiments, the lower surface temperature is $\sim$150 K, corresponding to a coverage of $\sim$0.63 ML. Well-ordered surfaces exhibiting CO in bridge (1955 cm^{-1}) and linear (2083 cm^{-1}) sites are observed (Fig. 1 and Table 1) by adsorbing CO above $\sim$270 K and cooling the surface in the presence of CO in the gas phase, in agreement with the literature [15]. When CO is adsorbed below $\sim$270 K, additional peaks appear (Fig. 1

Table 1
Frequencies of the various sites occupied by CO on Pd(111) in the temperature range 150–270 K (from Ref. [16])

	Sites of the normal structure		Sites populated in equilibrium with gas phase CO[a]		Extra sites populated by adsorption below 270 K[b]			
Type of site	Linear	Bridge	Linear	Three-fold hollow	Linear[c]	Linear	Bridge	Three-fold hollow[d]
Frequency[e] (cm^{-1})	2083	1955	2103	1890	2158	2093	1940	1890

[a] Observed only in equilibrium with gas phase CO above $\sim 10^{-6}$ mbar.
[b] Assigned to domain boundaries.
[c] Tentative.
[d] Three-fold hollow sites are observed only for an initial adsorption at a CO pressure larger than 10^{-6} mbar.
[e] The frequencies depend on the actual surface temperature and CO pressure.

and Table 1) at 2158 cm^{-1}, 2093 cm^{-1}, 1940 cm^{-1}, and 1890 cm^{-1} at the expense of the intensity of the regular peaks which are still present [16]. The overall intensity (sum of all the peak areas) is constant. The relative intensities of the extra peaks depend on the conditions of adsorption. They increase with the CO pressure that is used during the initial adsorption. The peaks at 1940 and 1890 cm^{-1} are not always measurably observed at our sensitivity. The peak at 2093 cm^{-1} overlaps the regular peak at 2083 cm^{-1}. The extra peaks were assigned to antiphase domain boundaries in Ref. [16]. The existence of antiphase domains had already been invoked to explain the large variation of the desorption kinetics with CO coverage [14]. The structure in the domains is identical to that of the annealed surface, so that the spectra still exhibit the 'normal' peaks of the linear and bridge sites, although with a smaller intensity. Domains nucleate only upon adsorption below $\sim$270 K, and they disappear by annealing above this temperature. The extra sites are populated with CO molecules below $\sim$230 K. Among the extra sites, the site at 2158 cm^{-1} which was already reported in Ref. [17] is most surprising, since its frequency is larger than in the gas phase [18]. It was suggested that this large frequency may result from a CO molecule occupying a distorted linear site and interacting with another linear CO on the next Pd atom [16]. An alternative possibility, not proposed in Ref. [16], is that the two interacting linear CO molecules are on the same Pd atom. This would give rise to one symmetric and one antisymmetric stretching modes, considerably split apart because of their large mutual interaction. In C_{2v} geometry, the antisymmetric mode would be forbidden [12], and therefore only one single band would result. In principle, this latter possibility is more unstable because of the repulsive interaction between the CO molecules. On the other hand, this configuration might result in less coupling with other COs and to the small observed bandwidth of 7 cm^{-1}.

In this work, photodesorption is investigated both at 308 nm with FTIR, and at 532 nm with sum frequency generation (SFG) as a probe. Since SFG uses picosecond lasers having a rather large peak power, a limitation in its applicability to measure populations of molecules in various sites may come from the laser induced thermal and/or photochemical desorption. CO on Pd(111) is a good case to investigate the laser desorption because it exhibits simultaneously strongly and weakly bound adsorption sites. On the other hand, non-thermal photodesorption occurs in general more easily for NO than for CO, and it does not occur for NO on Pd(111), suggesting that CO will not be photodesorbed from Pd(111). We do find that CO is not photodesorbed from Pd(111) if the CO adlayer is well ordered. It is only if the adlayer contains the extra sites that CO is observed to desorb, both at 308 nm and at 532 nm.

2. Experimental

The FTIR is used to probe the desorption induced by an excimer laser operated at 308 nm

(pulse duration $\sim$20 ns, fluence 9 mJ cm^{-2}, normal incidence), and the SFG is used to probe the desorption induced by a YAG laser (532 nm, $\sim$10 ps, 0.5 mJ cm^{-2}, angle of incidence: 54°, p-polarised). The beam uniformity of the excimer laser is evaluated by measuring the laser intensity through an aperture which is scanned in the beam at a point optically conjugated with the sample. It is found to be better than 10%. The uniformity of the YAG laser is not as precise, because the sample is a few centimetres in front of the focal point. As a result, the plane which is optically conjugated with the sample is not accessible. An iris diaphragm is placed in the beam at various points between the focusing lens and the sample. The laser power is measured as a function of the aperture and distance from the lens, allowing us to estimate both the fluence and the uniformity on the sample. The uniformity is found to be about 20%. The same YAG laser is used both for pumping and probing. This has two reasons. On the one hand, the objective is to find out whether the less bonded sites are stable enough under the laser beams used for SFG. On the other hand, we had no means in these experiments to vary the laser fluence without modifying slightly the alignment, which is crucial to probe the effect of the YAG laser by SFG. This is why we used the same fluence for pumping and probing. Although this procedure is not ideal, it can still be used provided that the desorption efficiency is negligible during the measurement of a SFG spectrum, and measurable over a time compatible with the stability of the experimental setup, which turned out to be the case.

The local laser heating is calculated by numerical integration of the heat flow equation [19,20]. It is found to be 17 K in both cases, with the difference that the heating lasts 35 ns (FWHM) in the case of the excimer, and only 50 ps for the YAG. Electron diffusion was not included in our calculation. It can be neglected only in the case of nanosecond pulses, and therefore the laser heating is significantly overestimated in the case of the YAG laser. Besides the local pulsed heating, a macroscopic CW heating may occur due to the accumulation of heat in the crystal and sample holder. We measured a heating of 30 K for 40 mW of radiation absorbed by the Pd crystal when the latter is not cooled by a liquid nitrogen flow. However, the heating is undetectable when the crystal is cooled (as is the case in the present experiments). The SFG experiments are done using the lasers of the CLIO (Collaboration pour un Laser Infrarouge à Orsay) facility of the LURE laboratory [21]. In the present work, we use an optical parametric oscillator (OPO) pumped by a mode locked, pulsed YAG laser. The IR beam ($\sim$10 ps, 2 mJ cm^{-2}, $\sim$1500 pulses per second, 2 cm^{-1} bandwidth) is scanned in the spectral region of the CO internal vibration. It is overlapped temporally and spatially on the Pd(111) single crystal with a frequency doubled fraction of the pump laser. The SFG is detected on a photomultiplier tube after passing through a combination of filters and monochromator used to reject the YAG and IR frequencies. The SFG from the sample is divided by the SFG obtained by mixing a small fraction of the laser beams into a ZnSe crystal. This introduces a slope in the baseline because the response of ZnSe is not entirely frequency independent. The IR laser path to the chamber is not purged against atmospheric water, and this results in a considerable noise below 1900 cm^{-1}, where the H_2O peaks are larger, despite the division by the signal from ZnSe. It results that the three-fold sites are not reliably observed in this experiment.

The FTIR experiments are performed in the same UHV chamber using a commercial Mattson spectrometer at a resolution of 4 cm^{-1}. The spectra are obtained after subtraction of a reference spectrum recorded before adsorption of CO. Since photodesorption experiments last a few hours, the limitation of our signal to noise ratio in FTIR experiments arises from long term fluctuations of the H_2O concentration in the path between the spectrometer and the detector. To minimise this effect, the subtracted reference spectrum is weighted by a factor which is typically in the range 0.95–1.05. This procedure however affects the noise of the spectra (because the subtraction is optimised to minimise H_2O lines and not to minimise the noise), and it also adds specific noise below $\sim$1900 cm^{-1} where H_2O lines are stronger (because H_2O lines are much larger than CO bands, the noise on the H_2O lines is comparable

to the CO band intensity). The three-fold hollow sites are strongly affected, and they are not quantitatively measured in this work, except when the peak is large (which occurs only when spectra are recorded with the surface in equilibrium with gas phase CO above 10^{-6} mbar: it is not the case during photodesorption). The low frequency side of the peak of the bridge sites around 1940 cm^{-1} is also affected, although to a much smaller extent. The other peaks are not directly affected, except through the noise added by subtracting the H_2O spectra. The difference spectra are less affected because they are recorded at smaller intervals, and because they are directly subtracted from one another without using a reference spectrum.

The Pd single crystal is prepared by Ar^+ sputtering at 1 kV and 350°C followed by several anneals at 500°C (the first one under 10^{-6} mbar of O_2). The cleaning method is checked in a preparation chamber by Auger electron spectroscopy and low energy electron diffraction. The surface temperature is measured by a thermocouple which is held firmly against the crystal.

3. Results

3.1. Excimer laser induced desorption probed by FTIR

No photodesorption is found when the CO layer is fully ordered. The results of a laser desorption experiment at 308 nm are shown in Fig. 2 for a CO layer adsorbed at 185 K. The laser desorption itself was made at 150 K. CO desorbs first from the three-fold and linear sites at 2093 cm^{-1} (Fig. 2b–a). It takes a much larger number of pulses to observe a significant decrease of the peak at 2158 cm^{-1} (Fig. 2c–b and d–c). The two normal peaks (linear sites at 2083 cm^{-1} and bridge sites) are not measurably photodesorbed, but the peak of the bridge sites shifts to lower frequencies during the initial desorption from the linear and three-fold sites, and not afterwards. Fig. 3 shows the evolution of the peak intensities as a function of laser pulse count. Under the assumption that the peak intensities are proportional to the density of CO molecules in the corresponding adsorption sites, the desorption efficiencies (defined as the fraction of the population in the adsorption site desorbed by one laser pulse) are extracted from Fig. 3, assuming an exponential decay of the peak intensities with laser count. They are $[6.1 \pm 0.4] \times 10^{-5}$ per pulse for the linear + three-fold hollow sites, $[5.1 \pm 0.6] \times 10^{-6}$ for the site at 2158 cm^{-1}, and $< 3 \times 10^{-7}$ for the regular bridge + linear sites. The error bars are twice the mean error provided by the fit.

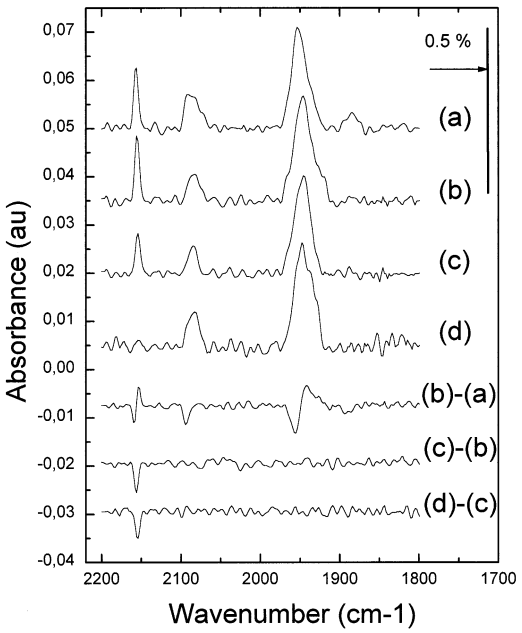

Fig. 2. Photodesorption at 308 nm and 9 mJ cm^{-2} in 20 ns probed by FTIR. The calculated laser heating is 17 K (peak temperature) and it lasts 35 ns (FWHM). The spectra are all recorded at 150 K without CO in the gas phase: (a) initial surface prepared by adsorption at 185 K under a CO pressure of 10^{-6} mbar. Note the broadening of the band of the linear sites at ~2083–2093 cm^{-1}, and the increased relative intensity of the peak at 2158 cm^{-1} with respect to the peak of the bridge sites at ~1950 cm^{-1}, when comparing with Fig. 1b (the larger the CO pressure during adsorption, the larger the number of extra sites); (b) after 5.4×10^4 laser pulses; (c) after 1.1×10^5 pulses; (d) after 3.1×10^5 pulses. The signal to noise ratio is better for the difference spectra (see text).

3.2. Calculation of laser heating and thermally induced desorption

We have calculated the transient surface heating induced by the excimer laser beam (Fig. 4). We

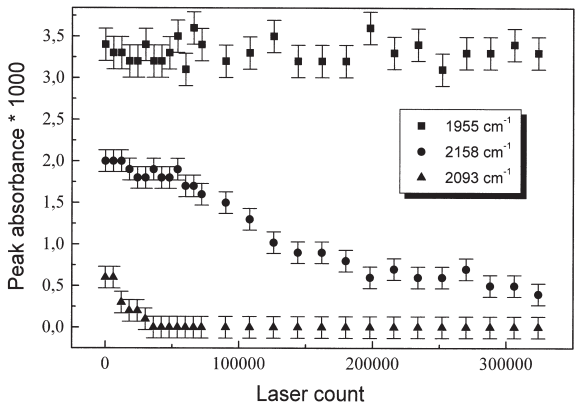

Fig. 3. Peak intensities measured by FTIR as a function of laser pulse count during exposure to the excimer laser beam (9 mJ cm^{-2}, 20 ns, 308 nm).

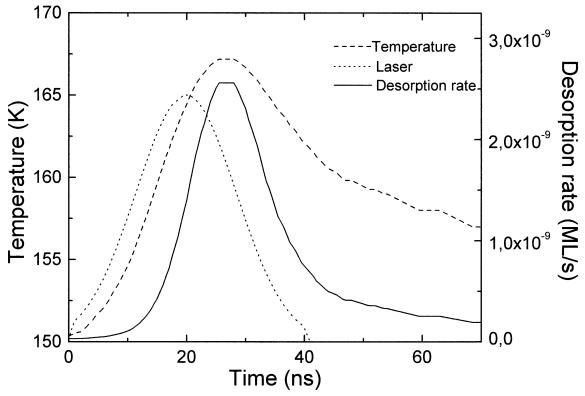

Fig. 4. Calculated laser induced temperature rise and corresponding thermal desorption rate of CO from Pd(111) induced by a laser of 9 mJ cm^{-2}, 20 ns at 308 nm. The laser temporal profile is also shown. The CO adsorption temperature is 200 K and the desorption temperature before a laser pulse is 150 K. The calculation is based on the numerical integration of the heat flow equation. The desorption kinetics are from Ref. [14]. The time integrated fraction of thermally desorbed molecules during the transient heating is 2.0×10^{-15} per laser pulse.

solve numerically the heat diffusion equation, using the code developed in our laboratory for studying laser heating of silicon in the conditions of laser etching [19,20]. This calculation is very precise because it is compared to the dynamics of heating and melting as measured through the Si reflectivity. The calculation is much more simple in the present case, where there is no phase transition, and where there are no strong variations of the thermal and optical coefficients with temperature. The computed laser induced heating is therefore reliable, providing that the spatial distribution of the energy in the laser beam is taken into account. As stated in the experimental section, the measured beam uniformity is better than 10%, the calculated temperature jump is 17 K, and it lasts 35 ns FWHM. The thermal desorption yield induced by laser heating can be calculated by integrating the desorption rate over the time of the temperature jump. The desorption parameters are taken from the work of Guo and Yates [14], who measured the desorption kinetics as a function of coverage for several adsorption temperatures down to 87 K. Fig. 5 shows that the set of desorption parameters allows us to calculate temperature programmed desorption (TPD) curves which are in quite reasonable agreement with Guo and Yates' TPD results [14]. The TPD curves exhibit four peaks (one of them visible only as a shoulder), at $\sim$275 K, $\sim$350 K, $\sim$400 K and 470 K, which correspond to the desorption from the linear+bridge (coverage>0.6 ML), compressed bridge alone (coverage between 0.6 and 0.5), bridge alone (coverage between 0.5 and 0.33 ML) and three-fold alone structures, respectively. A difference between the calculated and experimental curves is that the peaks are more visible in the calculated curves, perhaps because the desorption parameters vary stepwise and not continuously with coverage in the calculation. Since the desorption kinetics vary with adsorption temperature, we have calculated the thermal desorption efficiency induced by laser heating for different adsorption and desorption temperatures using the same parameters as for the TPD simulation (Table 2). Guo and Yates measured the desorption kinetics at 200 K and 87 K. We have assumed a linear variation of the desorption energy and logarithm of the pre-exponential factor when the adsorption temperature varies between 150 and 200 K at 0.63 ML. This is quite reasonable because Guo and Yates measured a quasi-linear dependence between 89 K and 200 K at 0.5 ML. The results of Table 2 show the extreme sensitivity of the thermal desorption kinetics with respect to both the adsorption and desorption temperatures. In all cases, the calculated thermal desorption yield is much smaller than the measured

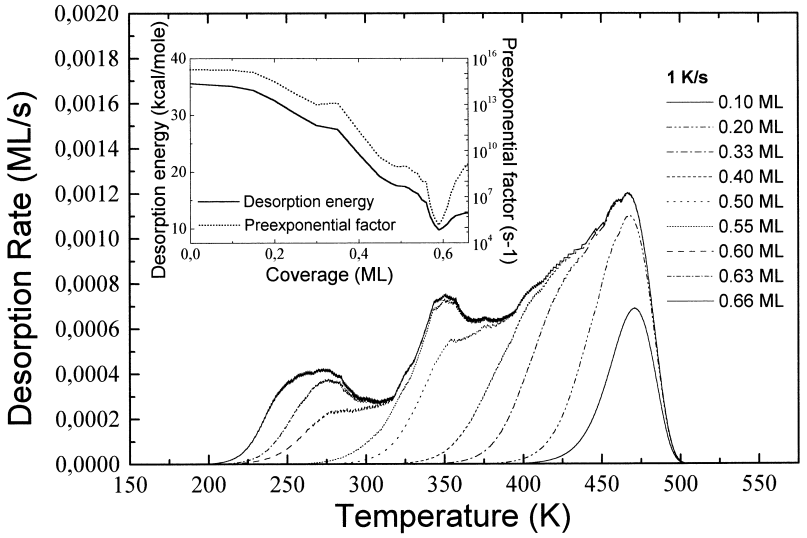

Fig. 5. Simulated TPD curves for various initial coverages of CO adsorbed at 200 K on Pd(111) for a heating rate of 1 K s^{-1}. The inset shows the kinetic parameters taken from Ref. [14] as a function of coverage. The same desorption parameters are used to calculate the laser desorption yield during one laser pulse.

Table 2
Calculated desorption efficiency per laser pulse induced by laser heating as a function of the adsorption and desorption temperatures for CO on Pd(111). Laser fluence 9 mJ cm^{-2}, laser wavelength 308 nm, pulse duration 20 ns

Adsorption temperature (K)	Desorption temperature (K)	Desorption efficiency
200	200	1.8×10^{-11}
200	150	2.0×10^{-15}
185	150	6.7×10^{-15}
150	150	1.2×10^{-13}

laser desorption yield. For the experimental conditions of Fig. 2, the calculated desorption efficiency is 6.7×10^{-15} per laser pulse: this calculated thermal yield is smaller than the experimental one by nine orders of magnitude. Such a difference cannot be ascribed to the assumptions made above. For example, a refined relationship between peak intensity and coverage cannot account for a discrepancy of nine orders of magnitude between the measured desorption yield and the calculated thermal desorption. It results that the laser desorption cannot be due to the thermal mechanism that is responsible for desorption in the TPD experiments.

3.3. Picosecond YAG laser induced desorption probed by SFG

As explained in the Introduction, photodesorption at 532 nm was also investigated under the conditions of the SFG experiments. The SFG spectrum (Fig. 6) shows the same peaks as the FTIR spectra of Fig. 1, with the difference that the peaks are slightly red-shifted and broadened in SFG. This difference between FTIR and SFG lineshapes was already observed in a number of cases. It is often interpreted as a consequence of an interference between the resonant SFG response of the adsorbate and the non-resonant SFG response of the substrate. The lineshape is particularly affected for CO/Pd(111), and the mentioned interference effect cannot explain the observed difference between FTIR and SFG: the interference could only produce the observed effect if the non-resonant intensity was comparable to the resonant intensity, which is far from being the case for CO/Pd(111) [22]. A more sophisticated theory of the SFG intensity is needed, but it is beyond the scope of the present work. Although a fully quantitative interpretation of our data would require this new theory, it is not necessary to evidence the

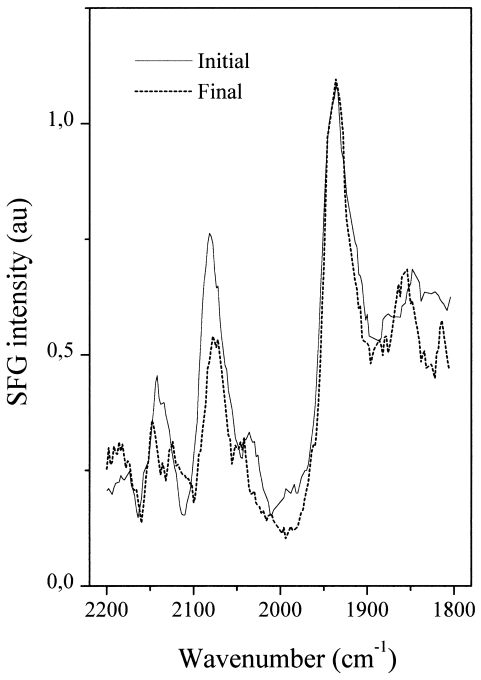

Fig. 6. Photodesorption at 532 nm and 0.5 mJ cm^{-2} in 10 ps probed by SFG. The laser heating is lower than 17 K (peak temperature) and it lasts 50 ps (FWHM). The spectra are all recorded without gas phase CO. Solid line: initial surface prepared by adsorption at 170 K under a CO pressure of 10^{-8} mbar. Dotted line: after exposure to 1.7×10^{7} laser pulses. The surface temperature was 150 K during the desorption experiment.

large effects of photodesorption which are clearly visible in the spectra of Fig. 6: after 1.7×10^{7} laser pulses at 532 nm, there is no measurable change of the peak assigned to the bridge sites, but the intensities of the other sites are much smaller: the YAG laser at 532 nm alone yields a selective desorption from the same sites as the excimer laser. The desorption efficiency is only $[3\pm1.5]\times10^{-8}$ per laser pulse at 532 nm. The corresponding desorption yield in a single SFG scan of 10 mn is $\sim$3%, which is at the level of the noise of our detection. This is sufficiently small to obtain spectroscopic information through the SFG spectra, even without gas phase CO in equilibrium with the surface, but it shows that attention must be paid to desorption when intensities corresponding to loosely bound molecules are measured.

The spectrum after readsorption (not shown in Fig. 6) is identical to the initial spectrum, showing that the photodesorption leaves the sites empty without further modification of the remaining CO layer. In particular, the photoexcitation does not produce a significant photodissociation of CO. Although the photodissociated fragments are not directly probed in the spectral region of the CO stretch, their presence would modify the local environment of CO molecules and therefore the vibrational spectrum.

The comparison of the desorption efficiencies due to the excimer and to the YAG is not straightforward, because the YAG has a pulse duration smaller than the excimer by a factor 2×10^{3}, and 30 times less photons per pulse. It makes more sense to compare desorption efficiencies per photon, taking into account the difference in

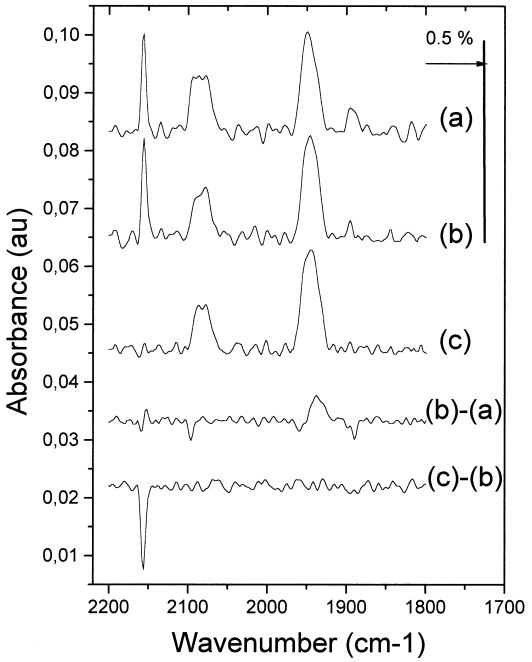

Fig. 7. Thermal desorption experiment probed by FTIR. The spectra are all recorded without gas phase CO: (a) initial surface prepared by adsorption at 150 K under a CO pressure of 5×10^{-6} mbar (note that the increase in CO pressure with respect to Fig. 2a has caused an increase of the relative intensities of the peaks at 2158 and 2083–2093 cm^{-1} with respect to the peak of the bridge sites at $\sim$1950 cm^{-1}); (b) after heating to $\sim$200 K and cooling to $\sim$160 K; (c) after heating to $\sim$230 K and cooling to $\sim$190 K. The signal to noise ratio is better for the difference spectra (see text).

reflectivity and absorption coefficient. The reflectivity of Pd is 0.698 at 532 nm and 0.537 at 308 nm. The coefficient of absorption is $8.74 \times 10^5\ cm^{-1}$ at 532 nm and $8.94 \times 10^5\ cm^{-1}$ at 308 nm: the difference between the absorption coefficients is therefore negligible. At $2158\ cm^{-1}$, the resulting efficiency per absorbed photon is $[1 \pm 0.2] \times 10^{-6}$ at 308 nm, and $[3 \pm 1.5] \times 10^{-8}$ at 532 nm. In general, it is found that short wavelengths and short pulses are more efficient to induce photodesorption: in both cases the excitation beats more easily the relaxation. It appears that the change of wavelength between 308 and 532 nm is quantitatively more important for CO/Pd(111) than the change of pulse duration from 20 ns to 10 ps.

In the case of the picosecond experiment, the calculated laser heating of 17 K is overestimated because the calculation does not include electron diffusion which is faster than heat diffusion at the picosecond time scale. The actual heating in our picosecond experiment is probably of a few Kelvin, and it lasts only 50 ps. Taking into account this difference of time scale only, and using the overestimated value of 17 K for the transient heating, the calculated thermal desorption per laser pulse is smaller than in the case of the excimer laser by a factor of 700: the thermal desorption mechanism measured by TPD cannot account for the laser desorption at 532 nm.

3.4. Thermal desorption

Figs. 7 and 8 show results of surface heating. The only difference in the preparation of the surface between Figs. 2 and 7 is the CO pressure during adsorption, that results in larger peaks for the sites associated with the domain boundaries in Fig. 7. The heating duration is chosen to observe the early stages of heating. The linear + three-fold hollow sites desorb at ~ 200 K and the site at $2158\ cm^{-1}$ desorbs at ~ 230 K. A difference between laser desorption and thermal desorption is visible in Fig. 7b–a with respect to Fig. 2b–a: interconversion from linear and/or three-fold hollow to bridge site seems to occur at the early stages of heating.

This is also apparent in the 'SFG-TPD' experiment of Fig. 8, where the IR frequency is held

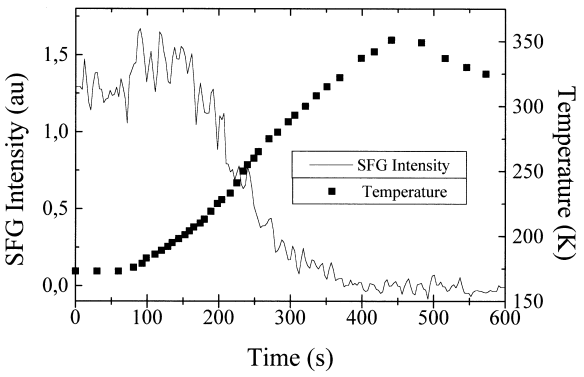

Fig. 8. Heating probed by SFG: the IR laser is tuned to the maximum of the peak of the bridge sites ($1940\ cm^{-1}$). The adsorption conditions are 180 K and 2×10^{-7} mbar. The SFG intensity and the surface temperature are recorded as a function of time.

fixed at the maximum of the peak of the bridge sites ($1940\ cm^{-1}$), while the surface temperature is increased at a rate of $\sim 0.5\ K\ s^{-1}$. This allows a site specific probe of thermal desorption, providing that the laser spectral width is larger than the width of the band to be probed. When using the CLIO free electron laser, the width may be as large as $50\ cm^{-1}$, making it possible to measure coverages as a function of time. In the present experiment we used the OPO of the CLIO facility which has a width of $\sim 2\ cm^{-1}$, so the intensity that we measure is not proportional to coverage, unless the peak shape of the band to be probed does not vary. The CO bridge site peak is always observed to broaden when the temperature increases. The minimal width is $\sim 20\ cm^{-1}$ for the fully ordered surface, and $\sim 30\ cm^{-1}$ in the presence of the extra sites. The width may increase up to $\sim 40\ cm^{-1}$ upon heating between 200 and 300 K. We expect therefore that the SFG signal, if probed at the peak maximum of the bridge sites, will decrease upon heating due to peak broadening and/or desorption, unless some interconversion takes place. However, an initial *increase* is observed upon heating from 175 to 205 K, and it can only be interpreted as the result of the interconversion from other sites to the bridge sites.

By further increasing the surface temperature (not shown in the figures), the peaks disappear sequentially. The linear sites at $2083\ cm^{-1}$ disap-

pear first. Then the bridge sites convert to three-fold hollow above ~ 380 K. These observations are consistent with the TPD curves of Fig. 5. Readsorption after heating leads to the regular surface (with no domains and no extra peaks) only if the temperature is raised above $\sim 300 \pm 30$ K.

4. Discussion

In summary, the CO adsorbed at the sites assigned to domain boundaries are the less stable, both by heating and by laser. There is no laser desorption from the regular sites. There is one minor difference between heating and laser desorption: interconversion to the bridge sites occurs thermally and not in photodesorption. The non-thermal nature of the photodesorption is supported by the numerical calculation of the thermal desorption yield induced by the transient laser heating. This calculation is based on detailed desorption kinetics measurements [14] and we were able to simulate accurately the TPD spectra of Ref. [14] with the same parameters that we used to estimate the contribution of thermal desorption in our photodesorption experiment. The difference between the calculated desorption induced by laser heating, and the experimental laser desorption is so large that it cannot originate from the various assumptions used or from the limitations in our signal to noise ratio. This means that the thermal desorption mechanism operative in TPD cannot be responsible for laser desorption. Thus, although the CO layer is critically dependent on temperature as shown by our heating experiments, by the calculations of Table 2, and by Guo and Yates' results, photochemical desorption must play a significant role in the present photodesorption experiments.

It is expected that at the frontiers between domains the molecules are displaced from their regular, most stable symmetric positions. Therefore the relative thermal instability of the CO molecules at these sites is not surprising. The interconversion to the bridge sites due to heating probably occurs by surface diffusion. Because the photon induced interconversion is negligible, it seems that in contrast the energy deposited in Pd:CO by photoexcitation is channelled very inefficiently into the motion of CO in the surface plane.

The photodesorption is qualitatively understood in the framework of the MGR mechanism [23]. Most of the photons excite primarily the solid, creating a distribution of photoelectrons with a wide distribution of energy that may attach temporarily to the adsorbates. In the case of CO, the electrons attach in the band formed by the 2π orbitals, which is almost empty. The energy transfer from the attached electron to the surface–adsorbate vibration and to the internal vibration of the adsorbate occurs because the molecular ion is formed out of its equilibrium position (with respect to the surface–adsorbate distance as well as to its internal coordinates). The observed absence of interconversion is probably due to the fact that the equilibrium position of CO in the plane of the surface is similar in the ground and excited states. The extent of the energy transfer is limited by the lifetime of the molecular ion, and only a small fraction of the attachments yield a photodesorption. In the case where the desorption fails, another electron attachment may occur before all the vibrational energy is transferred to the substrate. The desorption rate depends on (1) the rate of electron transfer, (2) the lifetime of the molecular ion, and (3) the desorption energy, which determines the minimal energy that must be converted from electronic to Pd–CO vibrational energy. The first factor favors strongly bound molecules, while the last two factors favor weakly bound molecules. The lifetime of the intermediate ion is the most critical parameter, since it is in general much shorter than the time of the substrate–adsorbate vibration (where the energy must be channelled for the molecule to desorb). If different sites differ only by the desorption energy, the molecule in the less bonded site desorbs more easily because it is more probable that enough energy will be converted during the lifetime of the excitation. It could be, however, that the adsorption sites also differ by the shape of potential energy surfaces, and therefore by the dynamics of the energy transfer. Thus, the fact that CO photodesorbs from Pd(111) from the less bonded sites is reasonable.

NO on Pt(111) seems to be a case similar to CO/Pd(111). The desorption rate at 193 nm increases by two orders of magnitude when NO is directly adsorbed at 80 K instead of being annealed to 220 K [6]. In the case of the annealed surface, NO at saturation occupies linear sites only, but weakly bound NO molecules are found in thermal desorption spectroscopy after exposure at 80 K [24,25]. In Ref. [6] NO is not probed by a site sensitive method, but the authors did speculate that weakly bonded NO was at antiphase domain boundaries. Photodesorption of CO from Pt(111) at 193 nm was also studied [3]. CO occupies linear sites on Pt(111) at low coverage, and a combination of linear and bridge sites at saturation. This suggests that the bridge sites are less bonded than the linear sites, but it is found that the desorption rate is at least four times smaller for bridge sites than for linear sites: CO/Pt(111) seems to be a case where less bonded sites are more difficult to photodesorb. This site sensitive effect is not comparable to the one that we observe, since it concerns the two sites of the regular structure, which are not observed to desorb on Pd(111) in this work. It is suggested in Ref. [3] that the difference in the desorption rates might be due to the different lifetime of the intermediate ion, in other words to the stronger coupling of the 2π CO orbital for bridge sites than for linear sites. The same behaviour was found for NO on Ag(111) and Cu(111) [5]. The absence of photodesorption from the regular sites of Pd(111) may be due to the longer wavelengths that we used, which result in a cooler energy distribution of the photoelectrons, and therefore to a smaller transfer rate to CO orbitals; more probably, it might be related to differences in the band structure of Pd and Pt above the Fermi level, which can modify the transfer rate of electrons from the metal to CO 2π orbitals.

5. Conclusion

We do not observe photodesorption of CO from the normal sites on Pd(111), but we do observe the photodesorption from defect sites assigned to antiphase domain boundaries. The desorption is more efficient at 308 nm than at 532 nm. Laser heating cannot account for the observed desorption efficiency. The difference between domains and boundaries can be due to the lower desorption energy at domain boundaries. The larger photodesorption rate for defect sites seems very similar to the case of NO on Pt(111). The absence of photodesorption from the regular sites may be due to the longer wavelengths (308, 532 nm) used in this work than in other studies of NO and CO on Pt(111) (193 nm), or to differences between Pd and Pt band structures above Fermi level. The present results also show that while weakly bound chemisorbed molecules can be detected by SFG in UHV, a weak laser induced desorption cannot be ruled out.

Acknowledgements

It is a pleasure to thank André Peremans for his assistance in the SFG experiments, and Georges Lefèvre for technical assistance. An anonymous referee is acknowledged for having proposed a second interpretation of the 2158 cm^{-1} band.

References

[1] K. Al-Shamery, H.-J. Freund, Curr. Opin. Solid State Mater. Sci. 1 (1996) 622.
[2] R.V. Kasza, J.G. Shapter, K. Griffiths, P.R. Norton, J.J. Sloan, Surf. Sci. 321 (1994) L239.
[3] K. Fukutani, M.-B. Song, Y. Murata, J. Chem. Phys. 103 (1995) 2221.
[4] S.K. So, R. Franchy, Z.C. Ying, W. Ho, J. Chem. Phys. 95 (1991) 1385.
[5] S.A. Buntin, L.J. Richter, D.S. King, R.R. Cavanagh, J. Chem. Phys. 91 (1989) 6429.
[6] K. Fukutani, Y. Murata, R. Schwarzwald, T.J. Chuang, Surf. Sci. 311 (1994) 247.
[7] M.-B. Song, M. Suguri, K. Fukutani, F. Komori, Y. Murata, Appl. Surf. Sci. 79/80 (1994) 25.
[8] T.T. Magkoev, M.-B. Song, K. Fukutani, Y. Murata, Surf. Sci. 330 (1995) L669.
[9] K. Ishikawa, J. Kanasaki, Y. Nakai, N. Itoh, Surf. Sci. 349 (1996) L153.
[10] X.H. Chen, J.C. Polanyi, D. Rogers, Surf. Sci. (1999) in press.
[11] F. Weik, A. de Meijere, E. Hasselbrink, J. Chem. Phys. 99 (1993) 682.
[12] F.M. Hoffmann, Surf. Sci. Rep. 3 (1983) 107.

[13] M. Tüshaus, W. Berndt, H. Conrad, A.M. Bradshaw, B. Persson, Appl. Phys. A 51 (1990) 91.
[14] X. Guo, J.T. Yates Jr., J. Chem. Phys. 90 (1989) 6761.
[15] J. Szanyi, W.K. Kuhn, D.W. Goodman, J. Vac. Sci. Technol. A 11 (1993) 1969.
[16] B. Bourguignon, S. Carrez, B. Dragnea, H. Dubost, Surf. Sci. 418 (1998) 171.
[17] W.K. Kuhn, J.S. Szanyi, D.W. Goodman, Surf. Sci. 274 (1992) L611.
[18] G. Herzberg, in: Molecular Spectra of Diatomic Molecules, I. Spectra of Diatomic Molecules, van Nostrand, New York, 1950, p. 522.
[19] B. Dragnea, J. Boulmer, J.-P. Budin, D. Débarre, B. Bourguignon, Phys. Rev. B 55 (1997) 13904.
[20] B. Dragnea, B. Bourguignon, Phys. Rev. Lett. 82 (1999) 3085.
[21] A. Peremans, A. Tadjeddine, W.Q. Zheng, P. Guyot-Sionnest, P. Remy, G. Ryschenkow, M. Buck, Y. Caudano, L.M. Yu, P.A. Thiry, B. Bourguignon, H. Dubost, B. Dragnea, S. Carrez, Nucl. Instrum. Meth. Phys. Res. A 375 (1996) 657.
[22] B. Dragnea, Ph.D. Thesis, University of Paris-Sud, Orsay, 1997.
[23] D. Menzel, Nucl. Instrum. Meth. Phys. Res. B 101 (1995) 1.
[24] J.L. Gland, B.A. Sexton, Surf. Sci. 94 (1980) 355.
[25] B.E. Hayden, Surf. Sci. 131 (1983) 419.